Chapter 5-Unsteady WSR Heat Release Model

A model must be created to examine how the system is impacted by the dynamics of the flame. The unsteady input comes from the acoustic particle velocity, while the unsteady heat release output provides forcing for the acoustics through the self-excited system outlined in chapter 1. With a dynamic model for the heat release, the system-based stability analysis can be completed by assembling the acoustics and flame with the proper scaling between each component. Figure 5.1 shows the input/output relationship for the flame dynamics of the system.

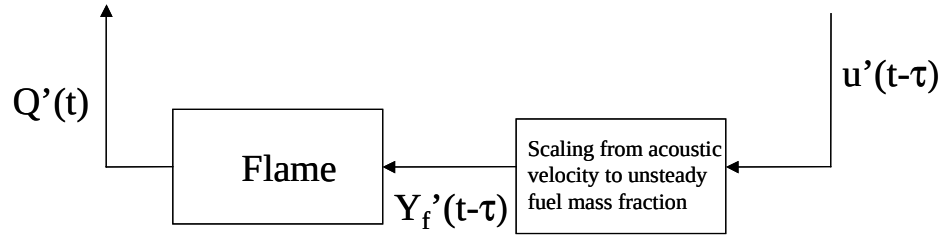

Figure 5.1-Partial block diagram showing the flame dynamics of the system.

5.1-WSR Model

A well-stirred reactor (WSR) models a simplified combustion process. Most of the work presented here is based on the model created by Fannin [5], which was used for system stability analysis on a similar test rig configuration. The purpose of this model is not to capture every detail of the combustion process, but rather to create a first generation flame model to gain a global understanding of the flame dynamics and the magnitude of the unsteady heat release.

5.1.1-Model Assumptions

The WSR model, described in Turns [32], has many simplifying assumptions which idealize the combustion process. The main assumption is that the properties of the reactor are uniform throughout which includes temperature, pressure, and species mass fractions. The model will be applied to Solar Turbine's single injector test rig which burns gaseous methane (CH_4) in a lean premixed swirl stabilized flame. Many simplifications were made to the combustion process in order to keep the problem

tractable. Figure 5.2 shows a schematic of an injector and a louver liner. Simplifications included the following assumptions:

1- Film cooling air does not participate in the combustion process.

2- The pilot diffusion flame is not included in the WSR model. The fuel used in the pilot is included in the equivalence ratio, and therefore the combustion process.

3- The F/A ratio is frozen from the fuel injection location to the flame front.

4- There is no heat transfer from the combustor control volume to the surrounding walls (adiabatic).

5- The control volume size is based on matching the computed equilibrium temperature and the steady-state fixed exit temperature.

6- A one-step global reaction mechanism was used where fuel+oxidizer =>products. The product enthalpy is calculated using a summation of enthalpies from the major products (CO, CO_2, HO, H_2O, O, O_2, N, N_2, NO, NO_2) whose equilibrium mass fractions are calculated by STANJAN.

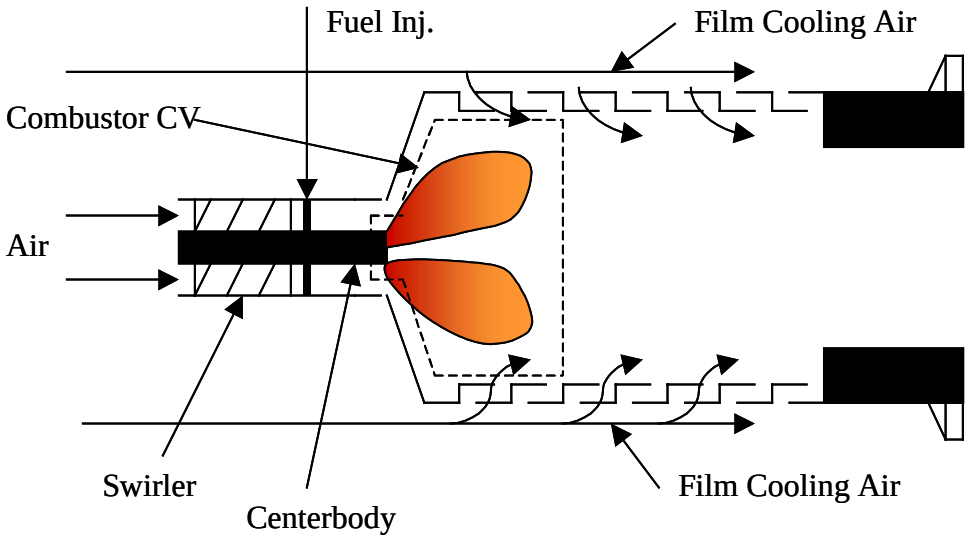

Figure 5.2-Schematic of a specific injector and combustion liner configuration.

5.1.2-Conservation Equations

Conservation of mass, momentum, and energy are the standard equations used to model any reacting flow system . Because the WSR model assumes steady-flow and constant pressure, the momentum equation is not needed in this model, but the WSR

model does require equations for the conservation of species and energy. Conservation of species is the reacting flow equivalent of conservation of mass in which the number of atoms are conserved. Mass is still conserved, although the chemical composition of the products leaving the CV is different from the reactants entering the CV due to the combustion process. Equation 5.1a shows the general species conservation equation. Stated in words, this equation says that the rate of change of a species mass inside the CV is equal to the species mass flow rate in, minus the species mass flow rate out, plus the mass generated inside the CV through a chemical reaction. With the assumption that the reactor is perfectly mixed, the value for the quantities leaving the control volume are equal to the quantities in the control volume.

Equation 5.1b shows the three species mass fraction (Y_i) conservation equations for the product and reactants. Realizing that the summation of all mass fractions must equal 1, only two dynamic equations are needed, with the product mass fraction (Y_{prod}) being described using a simple algebraic equation. The production rate term of fuel (ω_{fuel}) is derived using Arrehenius kinetics, with the pre-exponential factor and the activation energy found from empirical fits to experimental data under the assumption of a 1-step global reaction mechanism. The production rate of oxidizer is related to the production rate of fuel through the equivalence ratio ($\phi=((Y_{fuel}/Y_{oxid})/ (Y_{fuel}/Y_{oxid})_{stoic}$) of the reactants entering the control volume.

All of the time dependent variables are indicated as functions of time. These variables represent the states of the system ($Y_{fuel}(t)$, $Y_{oxid}(t)$, and $T(t)$), and the system inputs ($u_{in}(t)$, $u_{out}(t)$, and $Y_{fuel,in}(t)$). Fannin shows that the velocity inputs ($u_{in}(t)$ and $u_{out}(t)$) to the system are not really significant because the system response to these inputs are about the same magnitude with 180° phase difference between the two. Because of the phase difference, their impact on the dynamics of the system are negligible, and will be excluded from any further analysis. Assuming that combustion is taking place for $\phi<1$ (lean), and the molecular weight of the oxidizer being almost double that of methane, results in the mass fraction of air being nearly two orders of magnitude greater than that of the fuel. Thus, with small perturbations of the injector velocity the oxidizer mass fraction ($Y_{oxid,in}$) can still be considered constant, while the fuel mass fraction will be time varying ($Y_{fuel,in}(t)$).

$$\frac{dm_i}{dt} = \dot{m}_{in,i} - \dot{m}_{out,i} + \dot{m}_i''' V \quad (5.1a)$$

$$\rho V \frac{dY_{fuel}(t)}{dt} = \rho_{in} u_{in}(t) A_{in} Y_{fuel,in}(t) - \rho_{out} u_{out}(t) A_{out} Y_{fuel}(t) + MW_{fuel} \dot{\omega}_{fuel}(t) V$$

$$\rho V \frac{dY_{oxid}(t)}{dt} = \rho_{in} u_{in}(t) A_{in} Y_{oxid,in} - \rho_{out} u_{out}(t) A_{out} Y_{oxid}(t) + MW_{fuel} \frac{Y_{oxid,in}}{Y_{fuel,in}(t)} \dot{\omega}_{fuel}(t) V$$

$$Y_{prod} = 1 - Y_{fuel} - Y_{oxid}$$

$$\text{where } \dot{\omega}_{fuel}(t) = -(2.41E4 \frac{kmol}{kg\ s}) \rho Y_{fuel}^{.3}(t) (.233 Y_{oxid}(t))^{1.3} e^{\frac{-15098}{R_u T(t)}} \left[\frac{kmol}{m^3\ s} \right] \quad (5.1b)$$

The last conservation equation accounts for the energy transfer and generation through the control volume using a simplified version of the 1st law of thermodynamics (Equation 5.2a). Equation 5.2b shows that the rate of change in absolute enthalpy equals the absolute enthalpy entering the control volume minus that leaving the control volume. The absolute enthalpy formulation in Equation 5.3 is a combination of the enthalpy of formation, which accounts for the energy in the chemical bonds, and the sensible enthalpy, which accounts for the energy associated with the temperature of the species. Because of the 1-step global reaction mechanism all of the products are combined into one quantity. STANJAN was used to find the equilibrium concentrations of the major product species (CO, CO_2, HO, H_2O, O, O_2, N, N_2, NO, NO_2). Polynomial curve fits were obtained from Turns for each product species' absolute enthalpy. These were then combined with the equilibrium concentrations to find the product mixture enthalpy. All of the variables entering the control volume are evaluated at the inlet temperature, while all of the variables leaving the control volume are evaluated at the equilibrium flame temperature.

$$\rho V \frac{de}{dt} = \dot{m}_{in} h_{in,total} - \dot{m}_{out} h_{out,total} \quad (5.2a)$$

$$\rho V \frac{d}{dt}\left[\sum_{i=1}^{3}[h_i\, Y_i(t)] - (Y_{fuel}(t) + Y_{oxid}(t) + Y_{prod}(t))\frac{P}{\rho}\right] =$$
$$\rho_{in} u_{in}(t) A_{in}\left[h_{fuel,in} Y_{fuel,in}(t) + h_{oxid,in} Y_{oxid,in}\right] - \rho_{in} u_{out}(t) A_{out}\left[\sum_{i=1}^{3} h_i\, Y_i(t)\right] \quad (5.2b)$$

$$h = h_f + C_p \Delta T \quad (5.3)$$

5.1.3-Evaluation of Constants

All of the mean inlet and outlet constants such as density, velocity, pressure, etc… must be evaluated before the conservation equations can be solved. Solar Turbines provided actual test data for various mean velocities ranging from 97 ft/s to 68 ft/sec, and equivalence ratios from .67 to .50 as shown in Table 5.1. These operating conditions fixed the values of the inlet constants. The mean outlet conditions were found by evaluating the constants at the equilibrium temperature while maintaining continuity. The volume was adjusted for each operating condition so that the outlet temperature would match with computed equilibrium temperature. The volume of the reactor determines the residence time of the combustion process. A larger volume will allow for more complete combustion. Too small a volume will not allow enough time for ignition to occur, thus combustion will not take place. Choosing the reactor volume was very important given the assumption that the conditions inside the entire volume were uniform. In the analysis conducted by Fannin [5], CFD results were available to help estimate the value of the outlet temperature. Similar data for Solar's operating configuration was not available, so the outlet temperatures were estimated. In a crude sense, Fannin's outlet temperatures were approximately 3% below that of the adiabatic flame temperature, thus the outlet temperature of Solar's rig was fixed at 3% below the adiabatic flame temperature for each operating condition. Once an outlet temperature was chosen, the volume was adjusted in the model until the equilibrium solution resulted in a temperature equal to that of the outlet. Table 5.1 shows the volumes used and the percent of these volumes when compared to the total liner volume, excluding the volume of the plug in the louver liner case.

Event #	Inj. Vel	Inj. Vel.	Phi Dome	Yoxid	Yfuel	Tflame-adiab	Tflame-3%	Vol. of Comb	% of Entire Vol
(HOT)	(ft/sec)	(m/s)				(K)	(K)	(m^3)	
Louver Liner									
30	97.00	29.57	0.61	0.9655	0.0345	1913	1856	4.70E-03	50.0
31			0.62	0.9648	0.0352	1930	1872	4.42E-03	47.0
32			0.57	0.9676	0.0324	1844	1789	5.54E-03	59.0
33			0.56	0.9684	0.0316	1826	1771	5.73E-03	61.0
34			0.52	0.9708	0.0292	1754	1701	6.95E-03	74.0
14	83.00	25.30	0.60	0.9660	0.0340	1896	1839	4.13E-03	44.0
15			0.57	0.9675	0.0325	1844	1789	4.79E-03	51.0
20			0.56	0.9684	0.0316	1826	1771	4.89E-03	52.0
21			0.55	0.9689	0.0311	1808	1754	5.17E-03	55.0
16			0.55	0.9690	0.0310	1808	1754	5.17E-03	55.0
22			0.52	0.9706	0.0294	1754	1701	5.92E-03	63.0
17	78.00	23.77	0.67	0.9621	0.0379	2013	1953	3.01E-03	32.0
13			0.67	0.9623	0.0377	2013	1953	3.01E-03	32.0
18			0.63	0.9643	0.0357	1947	1889	3.48E-03	37.0
19			0.58	0.9675	0.0325	1861	1805	4.23E-03	45.0
23			0.52	0.9703	0.0297	1754	1701	5.54E-03	59.0
24			0.52	0.9706	0.0294	1754	1701	5.54E-03	59.0
25	68.00	20.73	0.65	0.9635	0.0365	1980	1921	2.82E-03	30.0
26			0.61	0.9656	0.0344	1913	1856	3.29E-03	35.0
27			0.58	0.9673	0.0327	1861	1805	3.66E-03	39.0
28			0.55	0.9688	0.0312	1808	1754	4.23E-03	45.0
29			0.52	0.9703	0.0297	1754	1701	4.89E-03	52.0
Backside Cooled Liner									
1	87.00	26.52	0.61	0.9656	0.0344	1913	1856	4.21E-03	31.0
2			0.56	0.9682	0.0318	1825	1770	5.03E-03	37.0
3			0.53	0.9698	0.0302	1772	1719	5.98E-03	44.0
4			0.50	0.9715	0.0285	1717	1665	6.93E-03	51.0

Table 5.1-Operating conditions and parameter values for test rig configuration with the louver liner w/ plug (P~9 atm and T_{inlet}~600K), and the backside cooled liner (P~7.8 atm and T_{inlet}~600K).

5.1.4-Formulation of Dynamic System

Remember that the purpose of this modeling process is to create a dynamic input/ouput relationship between the unsteady fuel mass fraction ($Y_{fuel,in}(t)$) and the unsteady heat release (Q'(t)). Three dynamic equations have been formulated to account for the dynamic behavior of the three system states ($Y_{fuel}(t)$, $Y_{oxid}(t)$, T(t)), with the system input ($Y_{fuel,in}(t)$) explicitly part of each equation. An equation relating the system states to the output must still be formulated. The heat release (Q) is composed of a mean and dynamic component, and can be easily found from the change in sensible enthalpy between the products and the reactants as shown in Equation 5.4. The enthalpy of formation is not included in the heat release because the formation energy is associated with chemical bonds and cannot be extracted from the system.

$$Q = \overline{Q} + Q'(t) = \rho u_{out}(t) A_{out} \sum_{i=1}^{3} Y_i(t) C_{p,i} (T(t) - T_{ref}) - \rho_{in} u_{in}(t) A_{in} (Y_{fuel,in}(t) C_{p,fuel} + Y_{oxid,in}(t) C_{p,oxid})(T(t) - T_{ref}) \quad (5.4)$$

The output equation completes the system formulation since now there is a defined relationship between the system input and the system output through the state equations. In general these equations can be manipulated in state space notation (Equation 5.5) which provides a compact representation of the system. The (N_x x 1) **x** vector represents the states of the system where N_x is the number of states. The (1 x N_u) **u** vector is the input vector which is a scalar for this system since there is only one (N_u=1) input. The (N_y x 1) **y** output vector is also a scalar since there is only one system output. The first equation represents the states' time rate of change as a function of the states through the (N_x x N_x) **A** matrix, and the input through the (N_x x N_u) **B** matrix. The second equation shows how the output depends on the value of the states through the (N_y x N_x) **C** matrix, and the input through the (N_y x N_u) **D** matrix. This notation is a standard form for a system of linear state equations, but in this case the system currently has non-linear components. As mentioned previously, the equations must be linearized in order to use linear analysis techniques, therefore the three dynamic equations and the output equation must be linearized before the entire system can be assembled and analyzed.

$$\begin{aligned} \dot{\mathbf{x}} &= \mathbf{A}\mathbf{x} + \mathbf{B}\mathbf{u} \\ \mathbf{y} &= \mathbf{C}\mathbf{x} + \mathbf{D}\mathbf{u} \end{aligned} \quad (5.5)$$

5.2-Conversion of Equations to State Space Form

In order to utilize the conservation equations derived above they must be linearized and put in a form which makes them applicable to performing a stability analysis. Stability is determined by applying a small perturbation to the system and seeing if the system damps the perturbation and returns it to its initial state, or whether the perturbation grows to produce large amplitude oscillations. Therefore, the analysis is conducted by adding small perturbations to the states of the system and then examining the stability of the linearized perturbed variables.

5.2.1-Linearization of the Conservation Equations

The first step in linearizing the conservation equations is to separate the rate terms from the rest of the terms. Equation 5.6 shows the conservation equations written in matrix notation. If both sides are pre-multiplied by $\mathbf{S^{-1}}$ then the rate terms become decoupled from the rest of the system with the **F** matrix becoming a coupled non-linear vector field which is a function of the system states and parameters. In order to linearize the system, the states and parameters are perturbed so that each has a mean and perturbed value as shown in Equation 5.7. These perturbed values are inserted into Equation 5.6. The equations are then expanded in a Taylor series where only the linear terms are retained. The equilibrium point around which the system is linearized is found by setting the rate terms to zero and solving for the roots ($\mathbf{x_0}^T;\mathbf{u_0}$) of the **F** matrix. ($\mathbf{F}(\mathbf{x}^T;\mathbf{u})=\mathbf{0}$).

$$\mathbf{S}(u_{in},u_{out},Y_{fuel,in})\begin{Bmatrix}\dot{Y}_{oxid}\\ \dot{Y}_{fuel}\\ \dot{T}\end{Bmatrix}=\mathbf{T}(\{Y_{oxid},Y_{fuel},T\}^T;u_{in},u_{out},Y_{fuel,in})$$

$$\begin{Bmatrix}\dot{Y}_{oxid}\\ \dot{Y}_{fuel}\\ \dot{T}\end{Bmatrix}=\mathbf{F}(\{Y_{oxid},Y_{fuel},T\}^T;u_{in},u_{out},Y_{fuel,in}) \quad (5.6)$$

$$\textit{where } \mathbf{F}=\mathbf{S}^{-1}\mathbf{T}$$

$$\begin{aligned}Y_{oxid}(t)&=\bar{Y}_{oxid}+Y_{oxid}'(t)\\ Y_{fuel}(t)&=\bar{Y}_{fuel}+Y_{fuel}'(t)\\ T(t)&=\bar{T}+T'(t)\\ u_{in}(t)&=\bar{u}_{in}+u_{in}'(t)\\ u_{out}(t)&=\bar{u}_{out}+u_{out}'(t)\\ Y_{fuel,in}(t)&=\bar{Y}_{fuel,in}+Y_{fuel,in}'(t)\end{aligned} \quad (5.7)$$

The Taylor series expansion is shown in Equation 5.8 in matrix notation. **D** is a matrix operator used to form a matrix of partial derivatives referred to as a Jacobian matrix. By definition, the $\mathbf{F}(\mathbf{x_0}^T;\mathbf{u_0})$ term is zero because it is the equilibrium solution. The remaining terms form the state space equation shown in Equation 5.5. The output equation must also be linearized in order to be used in a stability analysis. Expanding the

output equation in a Taylor series while keeping only the linear terms results in the linearized form of the output equation. Equation 5.9 shows how the Taylor series is implemented in matrix notation. The mean heat release equates with the mean term on the right hand side of Equation 5.9, leaving only the time varying terms which create the unsteady part of the heat release. Thus, through the linearization process, a state space formulation has been constructed which relates the unsteady mass fraction of fuel input to the unsteady heat release output.

$$\begin{Bmatrix} \dot{Y}'_{oxid} \\ \dot{Y}'_{fuel} \\ \dot{T}' \end{Bmatrix} = \mathbf{F}(\mathbf{x}_0^T;\mathbf{u}_0) + \mathbf{D_x F}(\mathbf{x}_0^T;\mathbf{u}_0) \begin{Bmatrix} Y'_{oxid} \\ Y'_{fuel} \\ T' \end{Bmatrix} + \mathbf{D_u F}(\mathbf{x}_0^T;\mathbf{u}_0) \{Y'_{fuel,in}\} + H.O.T.$$

$$\textit{where } \mathbf{D_x F} = \begin{bmatrix} \partial F_1/\partial x_1 & . & . & \partial F_1/\partial x_n \\ . & . & & . \\ . & & . & . \\ \partial F_n/\partial x_1 & . & . & \partial F_n/\partial x_n \end{bmatrix}, \mathbf{A} = \mathbf{D_x F}(\mathbf{x}_0^T;\mathbf{u}_0), \mathbf{B} = \mathbf{D_u F}(\mathbf{x}_0^T;\mathbf{u}_0) \tag{5.8}$$

$$\overline{Q} + Q'(t) = \mathbf{G}(\mathbf{x}_0^T;\mathbf{u}_0) + \mathbf{D_x G}(\mathbf{x}_0^T;\mathbf{u}_0) \begin{Bmatrix} Y'_{oxid} \\ Y'_{fuel} \\ T' \end{Bmatrix} + \mathbf{D_u G}(\mathbf{x}_0^T;\mathbf{u}_0) \{Y'_{fuel,in}\} + H.O.T. \tag{5.9}$$

$$\textit{where } \mathbf{C} = \mathbf{D_x G}(\mathbf{x}_0^T;\mathbf{u}_0), \mathbf{D} = \mathbf{D_u G}(\mathbf{x}_0^T;\mathbf{u}_0)$$

5.3-Modeling Results

A frequency response function (FRF) showing the dynamic relationship between an unsteady mass fuel fraction input and an unsteady heat release output can be obtained from the state space model previously generated. Figure 5.3 shows an FRF of the flame given a unity input. This system has 3 poles and 3 zeros, all of which are stable. For this operating configuration the poles are –94.9, -6.1, and -6.1 Hz. The general dynamic behavior of the flame makes sense based on a physical interpretation. The corner frequency of the FRF is mostly determined by the Arrehenius kinetics term. Because methane has relatively slow kinetics the flame can only respond to low frequency

changes. Fuels with larger Arrehenius terms would have more bandwidth and would begin to roll-off at a higher frequency.

The overall magnitude of the unsteady heat release is mostly determined by the pre-exponential factor of the one-step global reaction mechanism and the equivalence ratio. Fannin observed that the DC model gain was lower than expected when compared to the magnitude based on the mean variables. He found that small perturbations to the inlet fuel mass fraction produced 13 dB less DC gain in the model compared to heat release values based on the mean variables. This DC offset was seen for all of the operating conditions examined, therefore an additional 13 dB was added to the unsteady heat release magnitude. The shortcoming of the model seems to result from a lumping of all the products into one term. The DC offset was found by perturbing the equivalence ratio slightly. This perturbation will also slightly change the composition of the products, which can drastically change the product's sensible enthalpy because of the widely varying enthalpies of formation. The model computes the product enthalpy based on the equilibrium properties, therefore the model's prediction of the unsteady heat release will not capture the substantial change in sensible enthalpy for small fluctuations to the inlet fuel mass fraction. More dynamic equations, to keep track of the concentration of each specific product (CO, NO, N_2, etc…), would provide a more accurate value for the unsteady heat release.

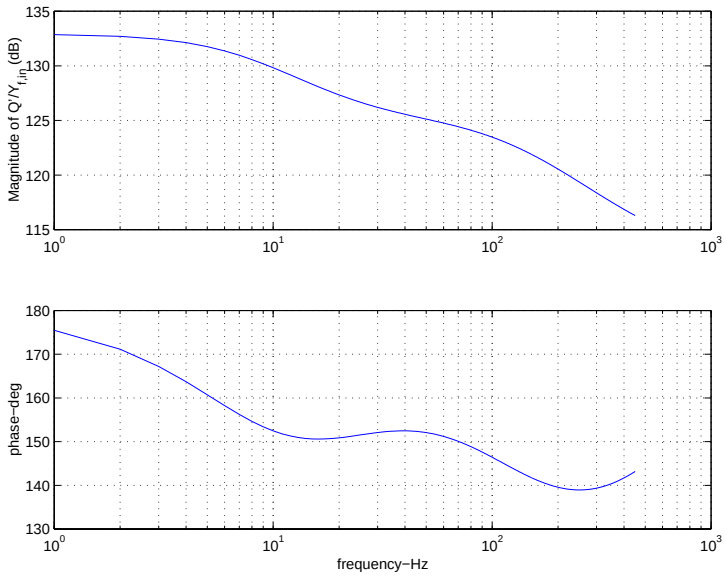

Figure 5.3-FRF of flame for $u_{inj,mean}$=97 ft/sec and ϕ=.52.

With 13 dB added, the magnitude of the flame FRF increases uniformly across the entire bandwidth. Figure 5.4 shows how the equivalence ratio affects the system response. There is very little change in the dynamics of the response since the pole values change very little with the equivalence ratio. The main affect of increasing ϕ is to increase the magnitude of the response. Since an increase in the equivalence ratio increases the amount of fuel available, one would expect to also see an increase in the amount of heat release.

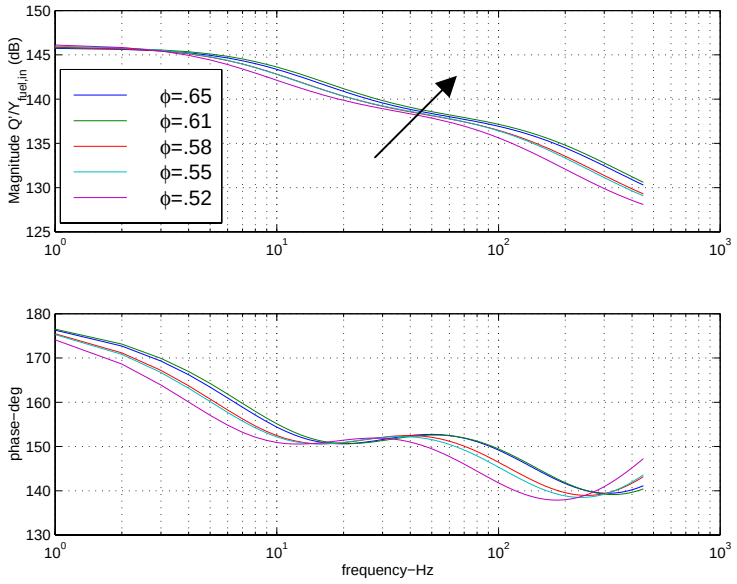

Figure 5.4-FRF of flame for various equivalence ratios. Arrow indicates direction of increasing equivalence ratios.

The other system parameter varied was the mean injector velocity. The major impact of the velocity is to change the delay time between the fuel injection location and the flame front. This matter will be discussed in the next chapter. Changing the mean velocity has very little affect on the dynamics of the flame, but because the mass flux through the reactor volume increases with increasing velocity, the magnitude of the flame response will increase with higher velocities as shown in Figure 5.5.

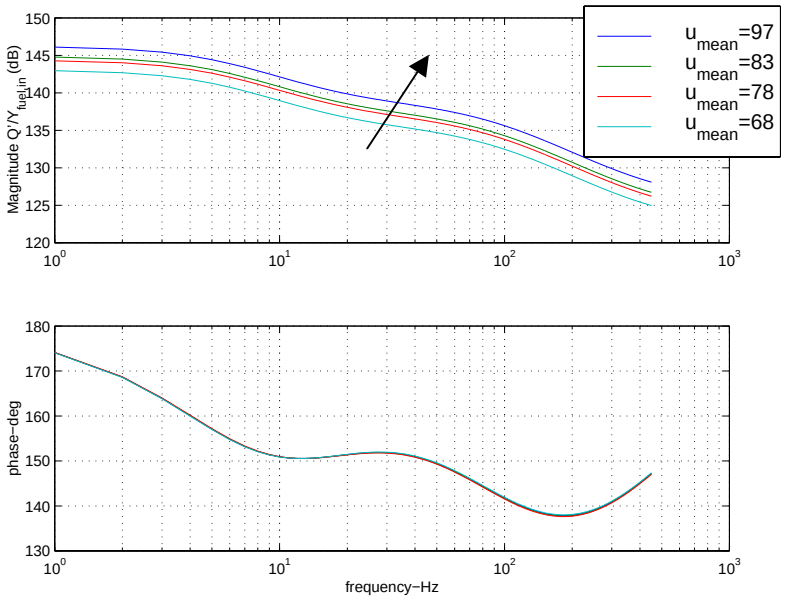

Figure 5.5-FRF of flame for various injector mean flow velocities and ϕ=.52. Arrow indicates direction of increasing velocity.

The purpose of this model was to develop a simplified dynamic input/output relationship between the unsteady fuel mass fraction and the unsteady heat release. From the analysis presented above, it can be seen that some of the simplifying assumptions are incorrect, but the analysis also shows that the main goals of finding an unsteady heat release gain, and the significant dynamics were achieved. Figures 5.4 and 5.5 show that the behavior of the flame responds as anticipated to specific changes in operating conditions, indicating that the model has captured the relevant physical phenomena of combustion. In order to complete the system analysis, the dynamic flame model will be inserted into the system loop with the acoustics, time delay, and the appropriate scaling in order to complete the system stability analysis. This process will be explained in the next chapter.